Vertical distribution of fluid velocity and suspended sediment in open channel turbulent flow

Article *in* Fluid Dynamics Research · June 2016

Impact Factor: 0.99 · DOI: 10.1088/0169-5983/48/3/035501

2 authors, including:

Debasish Pal

Singapore University of Technology and De…

10 PUBLICATIONS **14** CITATIONS

SEE PROFILE

Vertical distribution of fluid velocity and suspended sediment in open channel turbulent flow

2016 Fluid Dyn. Res. 48 035501

(http://iopscience.iop.org/1873-7005/48/3/035501)

IOP Publishing | The Japan Society of Fluid Mechanics Fluid *Dynamics* Research

Fluid Dyn. Res. **48** (2016) 035501 (27pp) doi:10.1088/0169-5983/48/3/035501

Vertical distribution of fluid velocity and suspended sediment in open channel turbulent flow

Debasish Pal and Koeli Ghoshal

Department of Mathematics, Indian Institute of Technology Kharagpur, Kharagpur 721302, India

E-mail: bestdebasish@gmail.com

Received 15 February 2015, revised 8 January 2016
Accepted for publication 9 January 2016
Published 7 March 2016

Communicated by Laurent B Mydlarski

Abstract

To predict the vertical distribution of streamwise fluid velocity and suspended sediment concentration profiles in an open channel turbulent flow, we derive a theoretical model here based on the Reynolds averaged Navier–Stokes equation and the mass conservation equations of solid and fluid phases. The model includes the effects of secondary current in terms of the vertical velocity of fluid, additional vertical velocity of fluid due to the suspended particles, mixing length of sediment-laden flow and settlement of the suspended particles due to gravitational force. We numerically solve our model as coupled differential equations and the obtained solution agrees well with a wide spectrum of experimental data. A detailed error analysis asserts the superior determination accuracy of our model in comparison to the traditional log-law and Rouse equation and other existing theoretical models. The significance of the turbulent features included in the model and the importance of their co-existence to compute velocity and concentration profiles are explained. In sharp contrast to the previous researchers, the present model has significant contribution in unveiling several latent phenomena of particle-turbulence interaction throughout the flow region. The model can also address various crucial phenomena of velocity and concentration profiles that occur during flow in real situation.

Keywords: open channel, turbulent flow, sediment concentration, secondary current, particle-turbulence interaction

1. Introduction

The transport of sediment in fluvial processes plays a significant role in geomorphic evolution such as dunes, river, estuarine morphology, coastlines etc and those evolutions have enormous importance in our practical life. Hence we have to gain an extensive knowledge on the sediment-laden flow mechanism for better forecasting of hydraulics related to fluvial geomorphology. The velocity of fluid along streamwise direction has the most significant role on the erosion and transportation of sediment. The highly fluctuating behavior of turbulent flow leads to an unpredictable nature of sediment dynamics in fluvial processes and therefore an immense effort is required to perceive this topic. Here we attempt to do a comprehensive theoretical study on the prediction of time averaged profiles of streamwise fluid velocity u and volumetric particle concentration c in suspension region to grasp a vivid knowledge on the sediment transport processes in open channel turbulent flow.

Researchers investigated the characteristics of u and c profiles through experiments and revealed the importance of particle-turbulence interaction, mixing of fluid and particle along vertical direction, secondary current, channel geometry etc in the mathematical modeling of those profiles. Prandtl (1932) and Rouse (1937) provided the analytical expressions on u and c profiles respectively; however those analytical expressions contain very few effects of turbulence and are only applicable to a limited range of turbulent conditions. The synchronization of u and c profile through a theoretical model is extremely tough owing to the highly fluctuating nature of the turbulent flow with sediment presence. This difficulty might be a reason that investigators either performed the theoretical investigation only on u profile (Umeyama and Gerritsen 1992, Guo and Julien 2001, Yang 2009, Kundu and Ghoshal 2012) or only that on c profile (Umeyama 1992, Huang *et al* 2008, Ghoshal and Kundu 2013, Kundu and Ghoshal 2013, 2014). It is worth mentioning that those models are constrained by the insufficient consideration of important turbulent effects and also were unable to reveal the underlying physics of particle-turbulence interaction in the flow region.

The determination of u and c profiles simultaneously through a theoretical approach is very essential as they are interrelated in the flow region. Also, this approach can unveil several latent phenomena of particle-turbulence interaction which play the most fundamental role to acquire a comprehensive knowledge on the turbulent flow dynamics laden with sediment. Very few theoretical investigations have been done on this topic owing to the complexity in modeling. Researchers (Tsai and Tsai 2000, Mazumder and Ghoshal 2002, 2006) theoretically determined u and c profiles together based on the mixing length approach and verified their models with the experimental data; however they avoided the investigation of particle-turbulence interaction in the flow region. Some models (Villaret and Trowbridge 1991, Ghoshal and Mazumder 2005, Herrmann and Madsen 2007) were developed on the aspect of sediment induced stratification and they explained a few physical insights on the interrelation between u and c profiles; nevertheless the models are limited due to several assumptions for getting a simplified mathematical form. Yang (2007) performed a mathematical analysis by considering secondary current in terms of the vertical velocity of fluid though his study provided insufficient explanation on the interaction of secondary current with u and c profiles in the flow region. The difficulty to apply each of the aforementioned mathematical models is the estimation of a large number of empirical parameters from the experimental data. The presumptive cause might be due to the exclusion of crucial turbulent effects and consequently a parameter which shows good estimation accuracy for velocity data has a high probability of failure to estimate concentration data with reasonable accuracy and vice versa. Also, those models considered the hindered settling phenomenon in terms of the particle Reynolds number whereas researchers (Cheng 1997a, Pal and

Ghoshal 2013) showed that the effect of sediment concentration needs to be embedded in this phenomenon. Besides this, some literature (Xingkui and Ning 1989, Guo and Julien 2001, Yang 2007, Castro-Orgaz *et al* 2012) revealed that the von Karman constant varies in sediment mixed fluid rather than its constant value in clear fluid and therefore its varying expression with concentration should be included in the modeling of u and c profiles. Overall, we can summarize that a generalized theoretical model needs to be developed by including several crucial effects of turbulence together with a few number of empirical parameters so that the model can provide us concise idea about the particle-turbulence interaction by revealing the underlying characteristics of u and c profiles together with their impacts on each other in the flow region.

This study attempts to solve the overlooked research problem mentioned. Here, we briefly state the organization of our research work. We start our mathematical modeling in section 2 based on the Reynolds averaged Navier–Stokes equation and the mass conservation equations of solid and fluid phases with the inclusion of (a) secondary current in terms of the vertical velocity of fluid, (b) additional vertical velocity of fluid due to the presence of sediment particles in suspension, (c) mixing length of sediment-laden flow, (d) von Karman constant of sediment-mixed fluid and (e) hindered settling phenomenon. Section 3 gives a detailed description on the consideration of experimental data from the published literature. Section 4 discusses the procedure of numerical solution of our model. Section 5 illustrates the comparison graphs between computed u and c profiles with experimental data and compares our model with the previously published models by an error analysis. Section 6 discusses the significance of the hydrodynamic mechanisms included in modeling, the importance of their co-existence, the contribution of the present model to uncover the latent phenomena of particle-turbulence interaction in suspension region and the advantage of our model in comparison to the existing ones from different points of view. The study is followed by a brief conclusion.

2. Mathematical model

For a fully developed open channel turbulent flow, we take the origin at the central region through the cross-sectional area of the open channel and the mutually perpendicular x, y and z axes through origin are considered along streamwise, vertical and lateral directions respectively. Assuming the steady state of the flow and its uniformity along x direction, we obtain the following equation from the continuity equation of fluid and the Reynolds averaged Navier–Stokes equation of turbulent flow

$$\rho_f \frac{\partial(uv)}{\partial y} + \rho_f \frac{\partial(uw)}{\partial z} = \rho_f g S + \mu_f \left(\frac{\partial^2 u}{\partial y^2} + \frac{\partial^2 u}{\partial z^2} \right) - \rho_f \left(\frac{\partial \overline{u'v'}}{\partial y} + \frac{\partial \overline{u'w'}}{\partial z} \right). \tag{1}$$

In equation (1), v and w are the time averaged velocities of fluid along y and z directions respectively, u', v' and w' are the velocity fluctuations of u, v and w respectively, ρ_f is the mass density of fluid, μ_f is the dynamic viscosity of fluid, g is the gravitational acceleration, S is the slope of the channel and the over bar indicates the time averaged value of the corresponding quantity. Guo and Julien (2001) showed the applicability of equation (1) for sediment-laden open channel flow. Rearrangement of equation (1) gives

$$\frac{\partial}{\partial y}\left[uv - \left(\nu_f \frac{\partial u}{\partial y} - \overline{u'v'}\right)\right] + \frac{\partial}{\partial z}\left[uw - \left(\nu_f \frac{\partial u}{\partial z} - \overline{u'w'}\right)\right] = gS. \tag{2}$$

At the central region through the cross-sectional area of the open channel, the variations of momentum flux $\rho_f uw$, viscous stress $\mu_f(\partial u/\partial z)$ and shear stress $-\rho_f \overline{u'w'}$ along z direction are negligible. Consequently, the magnitude of the second term in the left-hand side of equation (2) can be avoided in comparison to the magnitude of the first term of that side and we can write equation (2) as

$$\frac{\partial}{\partial y}\left[uv - \left(\nu_f \frac{\partial u}{\partial y} - \overline{u'v'}\right)\right] = gS. \tag{3}$$

Integrating equation (3), we obtain

$$uv - \left(\nu_f \frac{\partial u}{\partial y} - \overline{u'v'}\right) = gSy + k_1, \tag{4}$$

where k_1 is the integrating constant. To evaluate the expression of k_1, we use the following boundary condition

$$u(y_o) = 0 \text{ and } \left[\rho_f \nu_f \frac{\partial u}{\partial y} + (-\rho_f \overline{u'v'})\right]_{y=y_o} = \rho_f u_*^2, \tag{5}$$

where y_o is the vertical height from the bed surface at which $u = 0$ and $\rho_f u_*^2$ is the bed shear stress in which u_* is the shear velocity. Using equation (5), we obtain k_1 from equation (4) as

$$k_1 = -u_*^2 - gSy_o. \tag{6}$$

Inserting equation (6), we can rewrite equation (4) as

$$\nu_f \frac{\partial u}{\partial y} - \overline{u'v'} = uv + u_*^2\left(1 - \frac{gSy - gSy_o}{u_*^2}\right), \tag{7}$$

where y is the vertical height from the channel bed. In terms of channel slope S and flow depth h, we can write $u_*^2 = ghS$ and equation (7) is turned into

$$\nu_f \frac{\partial u}{\partial y} - \overline{u'v'} = uv + u_*^2\left(1 - \frac{y - y_o}{h}\right). \tag{8}$$

For sediment-laden open channel flow uniform along x direction, Yang (2007) proposed the mass conservation equation by adding the continuity equations of solid and fluid phases as

$$\frac{\partial(cv + \overline{c'v'} - c\omega_m)}{\partial y} + \frac{\partial(cw + \overline{c'w'})}{\partial z} = 0, \tag{9}$$

where c' is the fluctuation of c and ω_m is the settling velocity of the suspended particles in sediment-laden fluid. We neglect the second term of left-hand side in equation (9) by the same assumptions as equation (2) and perform integration of equation (9) to obtain

$$cv + \overline{c'v'} - c\omega_m = k_2 = 0, \tag{10}$$

where the integration constant k_2 is evaluated as zero by using the boundary condition that the mass flux is zero at the free surface of the open channel.

Yang (2007) proposed the following expression of Reynolds shear stress which can be obtained from equation (8) by applying $\nu_f = 0$ and $y_o = 0$

$$-\frac{\overline{u'v'}}{u_*^2} = \frac{uv}{u_*^2} + \left(1 - \frac{y}{h}\right). \tag{11}$$

Several researchers have inferred by experimental and theoretical investigations that all open channel flows are three-dimensional irrespective of the channel geometry and $v \neq 0$ due to the presence of secondary current (Yang *et al* 2004, Wang and Cheng 2005, Yang 2007, 2009). By analyzing experimental data (Muste and Patel 1997, Cellino and Graf 1999) of sediment-laden flow, Yang (2007) showed that the Reynolds shear stress deviates from its usual linear profile of clear fluid with an increasing value. From the aforementioned experimental observation and equation (11), he concluded that the increased Reynolds shear stress in sediment-laden flow is obtained either due to the decreased vertical velocity of fluid along downward direction whose magnitude along upward vertical direction increases or the suspended sediment particles contribute additional vertical velocity in fluid along upward direction and results increased $-\overline{u'v'}$ which is clear from equation (11). The explanation is modeled mathematically by Yang (2007) as

$$v = v_1 + v_2, \tag{12}$$

where v_1 is the vertical velocity of fluid without the contribution of suspended sediment and v_2 is the additional vertical velocity of fluid due to the presence of suspended particles. By inserting equation (12) into equations (8) and (10), we write the following equations

$$\nu_f \frac{\partial u}{\partial y} - \overline{u'v'} = uv_1 + uv_2 + u_*^2\left(1 - \frac{y - y_o}{h}\right), \tag{13}$$

$$\overline{c'v'} + cv_1 + cv_2 - c\omega_m = 0. \tag{14}$$

At this stage, we need to find appropriate expressions of v_1 and v_2 for solving equations (13) and (14). Nezu and Nakagawa (1984) performed experiment on the three-dimensional flow pattern and observed that secondary current, which is a combination of vertical and transverse velocities of the fluid, follows a circular motion along the cross-sectional area of open channel. Since we focus on the central region of the open channel along its cross-sectional area in this present study, the secondary current is considered in terms of the vertical velocity v_1 of fluid. The obtained results of Nezu and Nakagawa (1984) lead the boundary conditions of v_1 that it vanishes at channel bed and free surface of the open channel. On the basis of those boundary conditions, Yang (2005) proposed an expression of v_1 whose applicability is shown by Kundu and Ghoshal (2014) through the verification with the experimental data reported in literature (Ohmoto *et al* 2004, Wang and Cheng 2006). For an open channel flow containing sediment, we modify the formula of v_1 by replacing the von Karman constant κ of clear fluid to its expression κ_m for sediment-mixed fluid and propose the modified formula as

$$\frac{v_1}{u_*} = \lambda_1 \kappa_m \xi^{m_1}(1 - \xi)^{m_2}, \tag{15}$$

where $\xi (= y/h)$ is the normalized vertical height from the channel bed and λ_1, m_1, m_2 are parameters to be evaluated. From existing literature (Xingkui and Ning 1989, Guo and Julien 2001), we find that κ decreases with increasing particle concentration. To elucidate this fact, Yang (2007) gave a suitable mathematical expression on κ_m and its application for dilute and non-dilute sediment-laden flows is shown in Yang (2009). Hence, we select this expression which is given by

$$\kappa_m = \kappa\left(1 - \frac{0.14\, c^{\frac{1}{3}}}{c_m^{\frac{1}{3}} - c^{\frac{1}{3}}}\right), \tag{16}$$

where c_m is the maximum concentration of particle and it can be evaluated from the packing arrangement of particles in a certain domain. Equation (16) satisfies real condition by showing $\kappa_m = \kappa$ for particle free flow represented by $c = 0$ and by giving indefinite value at $c = c_m$ because at this state, the liquid flow region converts almost into solid region which is infeasible for the present study. We select the formula of v_2 given by Zhou and Ni (1995) as they derived it from solid and liquid volume flux rates with equal magnitude and opposite direction. They gave an explanation that the exchange rate of those phases along vertical direction must be in equilibrium due to the preservation of their incompressible properties during flow. The expression of Zhou and Ni (1995) is given by

$$v_2 = \frac{\omega_m c}{1 - c}. \tag{17}$$

The settlement of a particle along downward y direction is obstructed by the presence of other suspended particles. As a consequence, the settling velocity ω_m of the particle in sediment-laden fluid is reduced with increasing sediment entrainment and this phenomenon is known as hindered settling. To describe the physical characteristics of hindered settling, we select the following classic and widely cited expression of ω_m suggested by Richardson and Zaki (1954)

$$\omega_m = \omega_p(1 - c)^{n_H}. \tag{18}$$

In equation (18), ω_p is the settling velocity of particle in clear fluid and the exponent n_H measures the reduction of settling velocity in sediment-laden fluid. It can be seen that equation (18) expresses the actual behavior of settling velocity by giving $\omega_m = \omega_p$ for particle free flow given by $c = 0$.

To solve equations (13) and (14), explicit expressions of Reynolds shear stress $-\rho_f\overline{u'v'}$ and turbulent diffusion $-\overline{c'v'}$ are required. According to the theory of mixing length, we write the expression of $-\rho_f\overline{u'v'}$ as

$$-\rho_f\overline{u'v'} = \rho_f l^2\left(\frac{\partial u}{\partial y}\right)^2, \tag{19}$$

where l is the mixing length of the fluid in sediment-laden flow. It is defined by the characteristic length for which a fluid parcel conserves all its properties before mixing with the surrounding fluid. As this study deals with sediment-laden flow, it is essential to include the effect of suspended sediment in the expression of l. When more particles entrain in suspension, then the fluid at a particular vertical height coalesces with more particles at that height and moves less along vertical direction due to the heaviness of the lump of fluid and particle. This fact is mainly responsible for the reduction of l in sediment-laden flow in comparison to that in clear fluid. Umeyama and Gerritsen (1992) modeled this physical interpretation of l and here we use their expression which is as follows

$$\frac{l}{h} = \kappa_m\xi(1 - \xi)^{\frac{1}{2}\left(1+\lambda_2\frac{c}{c_a}\right)}, \tag{20}$$

where c_a is the reference concentration and λ_2 is an empirical parameter which is estimated from the experimental data. Furthermore, for more generalized expression of l, we modify κ of equation (20) by κ_m. The behavior of l mentioned before equation (20) can be understood well because its expression shows decreasing magnitude with increasing c for a particular ξ as $c \leqslant c_a$ and $0 \leqslant \xi \leqslant 1$. The turbulent diffusion term $-\overline{c'v'}$ in equation (14) is generally

expressed as

$$-\overline{c'v'} = \epsilon_s \frac{\partial c}{\partial y}, \tag{21}$$

where ϵ_s is the sediment diffusivity. It is expressed in terms of eddy viscosity ϵ_m by

$$\epsilon_s = \beta \epsilon_m, \tag{22}$$

where β is the inverse of the turbulent Schmidt number. If we look at equation (19), we can observe that $\partial u/\partial y$ depends on $-\rho_f \overline{u'v'}$ and l which include c through equations (11), (12), (15), (17) and (20). Hence, we include the effect of c through $\partial u/\partial y$ in the following well known expression of ϵ_m for open channel turbulent flow

$$\epsilon_m = u_*^2 (1 - \xi) \left(\frac{\partial u}{\partial y} \right)^{-1} \tag{23}$$

Using equations (16)–(20) in equation (13), the expression of normalized velocity gradient $\partial u^+/\partial \xi$ takes the form

$$\kappa^2 \left(1 - \frac{0.14\, c^{\frac{1}{3}}}{c_m^{\frac{1}{3}} - c^{\frac{1}{3}}} \right)^2 \xi^2 (1 - \xi)^{\left(1 + \lambda_2 \frac{c}{c_a}\right)} \left(\frac{\partial u^+}{\partial \xi} \right)^2 + \left(\frac{\nu_f}{u_* h} \right) \frac{\partial u^+}{\partial \xi}$$
$$- u^+ \lambda_1 \kappa \left(1 - \frac{0.14\, c^{\frac{1}{3}}}{c_m^{\frac{1}{3}} - c^{\frac{1}{3}}} \right) \xi^{m_1} (1 - \xi)^{m_2} - u^+ \frac{\omega_p}{u_*} c (1 - c)^{n_H - 1} - \left(1 - \xi + \frac{y_o}{h} \right) = 0, \tag{24}$$

where $u^+ (= u/u_*)$ is the normalized streamwise fluid velocity. The above equation is a quadratic equation of $\partial u^+/\partial \xi$ and the negative root is not feasible for open channel flow as it gives decreasing values of u^+ with increasing ξ. Therefore, we consider the positive root of equation (24) and finally $\partial u^+/\partial \xi$ is given by

$$\frac{\partial u^+}{\partial \xi} = \frac{-f_2 + \sqrt{f_2^2 - 4 f_1 f_3}}{2 f_1}, \tag{25}$$

where the expressions of f_1, f_2, and f_3 are written as

$$f_1 = \kappa^2 \left(1 - \frac{0.14\, c^{\frac{1}{3}}}{c_m^{\frac{1}{3}} - c^{\frac{1}{3}}} \right)^2 \xi^2 (1 - \xi)^{\left(1 + \lambda_2 \frac{c}{c_a}\right)}, \tag{26}$$

$$f_2 = \frac{\nu_f}{u_* h}, \tag{27}$$

$$f_3 = -u^+ \lambda_1 \kappa \left(1 - \frac{0.14\, c^{\frac{1}{3}}}{c_m^{\frac{1}{3}} - c^{\frac{1}{3}}} \right) \xi^{m_1} (1 - \xi)^{m_2} - u^+ \frac{\omega_p}{u_*} c (1 - c)^{n_H - 1} - \left(1 - \xi + \frac{y_o}{h} \right). \tag{28}$$

On the other hand, inserting equations (16)–(18) and equations (21)–(23) into equation (14), we write the expression of normalized concentration gradient $\partial c/\partial \xi$ as

$$\frac{\partial c}{\partial \xi} = \left[\frac{\lambda_1 \kappa \left(1 - 0.14 \dfrac{c^{\frac{1}{3}}}{c_m^{\frac{1}{3}} - c^{\frac{1}{3}}}\right) c \xi^{m_1} (1 - \xi)^{m_2}}{\beta (1 - \xi)} + \frac{\omega_p}{u_*} \frac{c(2c - 1)(1 - c)^{n_H - 1}}{\beta (1 - \xi)} \right] \frac{\partial u^+}{\partial \xi}. \tag{29}$$

To solve the derived system given by equations (25) and (29), suitable expressions for the turbulent components y_o, ω_p and n_H are needed to be chosen. In available literature, we find very few expressions of the vertical height y_o from the channel bed surface at which $u = 0$ and we take its following formula from Herrmann and Madsen (2007) which is widely cited and shows good agreement with the experimental data.

$$y_o = \frac{D}{30}[4.5(\tau_* - \tau_{*c}) + 1.7], \tag{30}$$

where D is the particle diameter, τ_* is the normalized shear stress and τ_{*c} is the normalized critical shear stress. The widely used expression of τ_* is written as follows

$$\tau_* = \frac{u_*^2}{\Delta_p g D}, \tag{31}$$

where $\Delta_p = (\rho_p - \rho_f)/\rho_f$ in which ρ_p is the mass density of particle. For the incipient motion of the particle at the channel bed, τ_{*c} plays the most important role. To avoid the trial and error estimation of the threshold bed shear stress for the incipient motion of particle, Soulsby and Whitehouse (1997) proposed a simple and widely applicable formula of τ_{*c} in terms of normalized particle diameter D_* by

$$\tau_{*c} = \frac{0.24}{D_*} + 0.055[1 - \exp(-0.02 D_*)], \tag{32}$$

where D_* is given as

$$D_* = \left(\frac{\Delta_p g}{\nu_f^2}\right)^{\frac{1}{3}} D. \tag{33}$$

Falling under the influence of gravity, a particle in stagnant clear fluid reaches a constant velocity called settling velocity ω_p when the sum of all upward forces equals to the downward weight of that particle. From the vast literature available on this turbulent feature, some expressions (Cheng 1997b, Ahrens 2000, Guo 2002, Jimenez and Madsen 2003) are used extensively. We select the following advanced formula of ω_p proposed by Zhiyao *et al* (2008) as it shows good agreement for a wide range of experimental observations and provides least error in comparison to the existing ones which are used frequently

$$\omega_p = \frac{\nu_f}{D} D_*^3 \left[38.1 + 0.93 D_*^{\frac{12}{7}}\right]^{-\frac{7}{8}}. \tag{34}$$

Equation (18) connects ω_p to the settling velocity ω_m of particle in sediment-mixed fluid by n_H and c. So a correct determination of ω_m depends on an appropriate choice of n_H. We follow that most of the old formulae of n_H (Richardson and Zaki 1954, Garside and Al-Dibouni 1977) were expressed as a function of the Reynolds number $\mathrm{Re}(=\omega_p D/\nu_f)$ of particle. During sediment-laden flow, particles move randomly in fluid and collide to each other. Though Cheng (1997a) took the effect of c in his expression of n_H, but he avoided the

effects of particle-fluid and particle-particle interactions which play significant role in the determination of n_H. Pal and Ghoshal (2013) suggested n_H by incorporating those effects and a concept of apparent particle diameter which is defined by the diameter of the apparent spherical volume where the particle whose settling velocity is to be evaluated can move randomly after colliding with other suspended particles in that volume. The expression of n_H is valid for a wide range of c and it provides least error in comparison to the other published models (Richardson and Zaki 1954, Garside and Al-Dibouni 1977, Cheng 1997a). So, the following formula of n_H by Pal and Ghoshal (2013) is selected for this study

$$n_H = \frac{\frac{4}{3}\ln(1-c) - \ln\left(1-\frac{c}{c_m}\right) + 3\ln f_h - \frac{7}{8}\ln\left[\frac{38.1 + 5.74 f_h^{\frac{12}{7}}\mathrm{Re}^{\frac{4}{7}}}{38.1 + 5.74\mathrm{Re}^{\frac{4}{7}}}\right]}{\ln(1-c)}. \tag{35}$$

Pal and Ghoshal (2013) suggested f_h in equation (35) as

$$f_h = \left[\frac{(1+\Delta_p)(1-c)^{\Delta_p} - 1}{\Delta_p}\left(1-\frac{c}{c_m}\right)^2 (1-c)^{-1}\right]^{\frac{1}{3}}. \tag{36}$$

Towards the end of mathematical modeling, to solve equations (25) and (29), the boundary condition required is that at $\xi = \xi_a$, $u^+ = u_a^+$ and $c = c_a$ where $\xi_a = a/h$ in which a is the dimensional reference level or the bed load layer thickness, $u_a^+ = u_a/u_*$ in which u_a is the dimensional reference velocity and c_a is the reference concentration which is defined by the equilibrium near-bed concentration between bed load and suspended load. As a locates the equilibrium position between bed load and suspended load, its position is very near to the bed and we select it as $0.02h$ which is quite reasonable. Suitable expression on u_a^+ is still lacking in literature and therefore it is estimated from the experimental data. Only a few expressions (Smith and McLean 1977, Garcia and Parker 1991, Zyserman and Fredsoe 1994) are available on c_a and most of them either provide underestimated or overestimated value in comparison to its expected value. According to the physical definition of c_a, Cao (1999) evaluated it by balancing the sediment entrainment based on the turbulent bursting and the deposition of suspended sediment near the bottom boundary of flow region. He verified his model with a wide range of experimental data with various bed forms which are observed generally over the channel bed during experiment. Since the formula of Cao (1999) provides quite reasonable value of c_a, we select its expression and is given by

$$c_a = \frac{0.6}{160}\frac{U_m}{\omega_p}\frac{D}{h}\frac{\tau_* - \tau_{*c}}{\tau_{*c}}\left(\frac{D\sqrt{\Delta_p g D}}{\nu_f}\right)^{0.8}, \tag{37}$$

where U_m is the mean streamwise fluid velocity throughout the flow depth.

Equations (25) and (29) together with the above mentioned boundary condition are solved to compute the vertical distribution of u and c profiles in open channel turbulent flow laden with sediment.

3. Experimental data considered for verification

Here we discuss the selection of experimental data from published literature to verify our model given by equations (25) and (29). The derivation of our model includes l, ω_p, n_H and κ_m which are the imperative elements for modeling of sediment-laden flow according to the modern research. Furthermore, secondary current plays a crucial role in our model and the

Table 1. Summary of experimental data and the estimated values of unknown parameters.

Run	D (mm)	h (cm)	U_m (cm s^{-1})	u_* (cm s^{-1})	Δ_p	u_a^+	λ_2
			Vanoni (1946)				
1	0.16	14.8	100.64	6.00	1.65	9.8	3.5
3	0.16	15.1	107.29	6.10	1.65	8.3	15.7
5	0.16	15.1	106.07	6.10	1.65	7.4	19.1
6	0.16	15.8	120.70	6.22	1.65	8.9	17.6
7	0.16	15.2	108.51	6.10	1.65	8.1	19.6
8	0.16	14.7	115.52	6.00	1.65	8.3	22.3
9	0.16	9.2	91.74	4.75	1.65	9.1	21.5
11	0.16	14.4	117.35	5.94	1.65	8.4	30.2
12	0.16	9.1	89.31	4.72	1.65	8.3	30.5
13	0.16	14.6	85.65	5.97	1.65	9.3	19.6
15	0.16	8.4	77.42	4.51	1.65	7.3	22.1
16	0.16	16.4	82.30	4.48	1.65	9.0	18.5
18	0.10	14.1	75.59	4.14	1.65	8.7	7.3
19	0.10	7.2	54.86	2.97	1.65	9.3	9.6
20	0.10	14.1	98.75	5.88	1.65	8.4	2.6
21	0.10	7.1	69.49	4.14	1.65	8.4	1.5
22	0.13	9.0	79.25	4.69	1.65	8.6	6.5
			Lyn (1988)				
1565EQ	0.15	6.4	64.90	3.58	1.65	7.9	25
1957ST-1A	0.19	5.7	71.80	3.74	1.65	9.5	30
1957ST-1B	0.19	5.7	73.60	3.69	1.65	11.8	10
			Xingkui and Ning (1989)				
SQ1	0.15	8.0	187.00	7.37	1.65	16.8	2.2
SQ2	0.15	8.0	187.00	7.40	1.65	15.1	5.5
SQ3	0.15	8.0	185.00	7.37	1.65	14.8	6.3

prediction of its effect in the flow region is a topic of concern throughout the previous few decades. Therefore we have to select experimental runs where the secondary current significantly influences u and c profiles.

Vanoni (1946) performed experiments in an 18 m long and 84.5 cm wide recirculating flume with an artificially rough bed surface made by sands. He observed that the spanwise distribution of particles is changed periodically and presumed that the reason is due to the appearance of secondary current. The presumption of Vanoni (1946) was confirmed by several researchers (Kinoshita 1967, Imamoto and Ishigaki 1988, Nezu 2002); so we collect seventeen experimental runs of Vanoni (1946) for the verification of our model.

Several researchers (Yang *et al* 2004, Yang 2005, Absi 2011) revealed that the effect of secondary current is very prominent for narrow open channel where the aspect ratio $A_r\,(=b/h)$ is less than 5, b being the width of the channel. As we already have considered seventeen experimental runs of Vanoni (1946), we want to select experimental runs for narrow open channel also. In a narrow open channel with 26.7 cm width, Lyn (1988) performed experiment with equilibrium and starved beds. This fact attracts us to verify our model with the data where both secondary current and variation of bed together are present. Out of all the experimental data of Lyn (1988), we select three runs in which one is for equilibrium

bed and other two are for starved bed. Xingkui and Ning (1989) performed experiment in a narrow open channel with width 30 cm and for sand particle, they collected three experimental runs in which the amount of sediment was increased gradually. We select those three runs for the verification of our model as the concentration of particles plays significant role for each effect considered in our study.

Table 1 shows a summary of wide experimental data considered for the verification of our model. We also provide the estimated values of u_a^+ and λ_2 for each run in table 1 and their estimation processes are discussed in the next section.

4. Procedures of numerical solution

Equations (25) and (29) are a system of two differential equations and the analytical solution of this system is not possible. To solve them numerically, we adopt explicit fourth order Runge–Kutta method due to its good prediction accuracy. It needs to mention that the unknown values of c_m, β, m_1, m_2, λ_1, u_a^+ and λ_2 are required to get the numerical solution of u and c profiles. As the diameter of a particle is computed from the equivalent volume of spherical particle, a suitable packing arrangement where spherical particles have crucial role needs to be chosen for computing the maximum concentration c_m of particle. We select its value as $2/3$ evaluated by Cheng (1997a) through arranging identical spheres in a cylinder with unit length and the diameter which equals to the diameters of used spheres. The competent choice of β is very important due to its physical importance. We select the following widely cited expression of β given by van Rijn (1984) as it provides suitable value for a wide range of grain-sizes

$$\beta = 1 + 2\left(\frac{\omega_p}{u_*}\right)^2. \tag{38}$$

The values of m_1 and m_2 in equation (15) are taken as 1 as they provide adequate determination accuracy to compute v_1 and this fact is proved by previous researchers (Yang 2005, Ghoshal and Kundu 2013, Kundu and Ghoshal 2014). Yang *et al* (2004) modeled the vertical velocity v_1 of fluid by $uv_1/u_*^2 \propto -\xi$ and proposed the proportionality parameter in this equation as a function of lateral length z from the sidewall. In our model, u and c are computed at the central region of the channel through the cross-sectional area i.e. $z = b/2$. During the computation of u and c profiles, we examine the performance of the proportionality parameter given by Yang *et al* (2004) and it provides fruitful result. Therefore, the expression of λ_1 for this study is taken by

$$\lambda_1 = 1.3 \exp\left(-\frac{b}{2h}\right). \tag{39}$$

The values of normalized reference velocity u_a^+ and λ_2 are required for the numerical solution of our model. The expressions available in literature on those parameters are very few and they do not provide suitable outcome for a wide range of turbulent flow; so those parameters are estimated from experimental data. In several published models (Tsai and Tsai 2000, Mazumder and Ghoshal 2002, Ghoshal and Mazumder 2005, Mazumder and Ghoshal 2006, Yang 2007), researchers calculated u_a^+ at ξ_a by either interpolation or extrapolation method from experimental data and this estimation process is very common. In this context, we want to mention that sometimes a profile of measured experimental data depicts inconsistent behavior due to the irregular nature of turbulence and erroneous value of u_a may be obtained from interpolation and extrapolation method. This inaccurate result may lead to

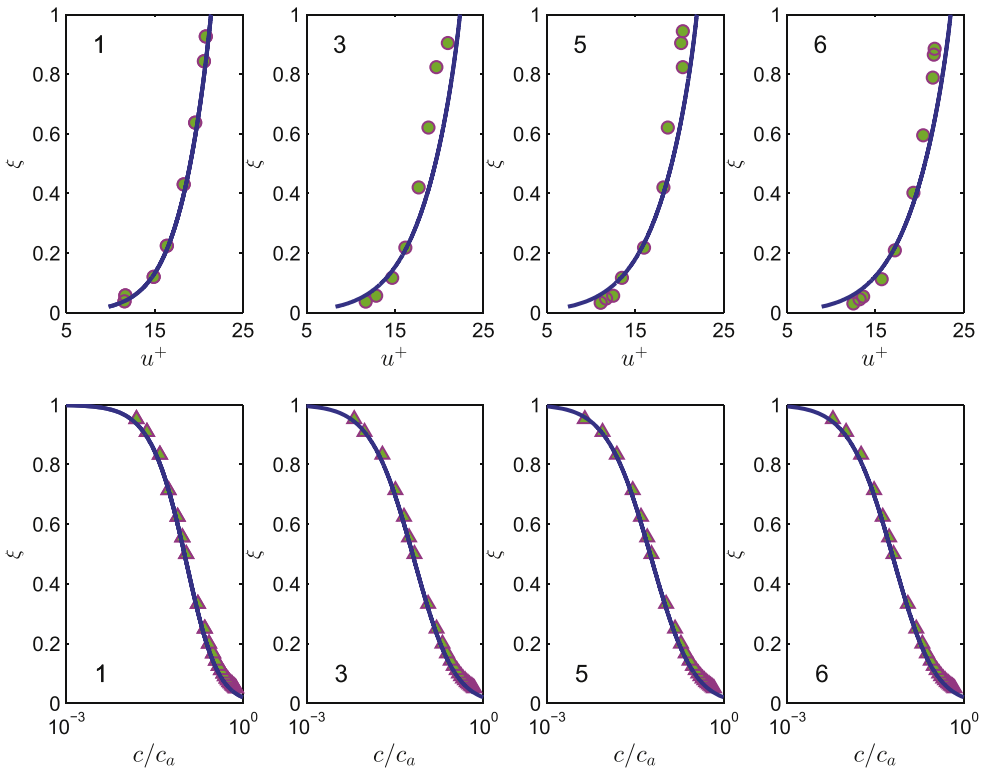

Figure 1. For experimental runs 1, 3, 5 and 6 of Vanoni (1946), comparison of u and c profiles between measured data (symbol) and computed values (solid line) from equations (25) and (29).

error in computing u and c profiles. Hence we estimate u_a from experimental data instead of doing interpolation or extrapolation. For each experimental run, the values of u_a^+ and λ_2 are evaluated as follows. The location of $a = 0.02h$ in this study is very near to the channel bed. So a rough initial estimation of u_a^+ at $\xi_a = 0.02$ is calculated through the extrapolation method from measured u data. The primary value of λ_2 is considered as 1. The numerical solution of equations (25) and (29) is started with those values of u_a^+ and λ_2. For each experimental run, we evaluate the final values of u_a^+ and λ_2 until a good matching is observed between computed and observed profiles of u and c simultaneously. The final estimated values of u_a^+ and λ_2 for each run are shown in table 1. We observe that the range of λ_2 obtained agrees with the existing ranges in literature (Umeyama and Gerritsen 1992, Umeyama 1992, Tsai and Tsai 2000, Ghoshal and Mazumder 2005, Mazumder and Ghoshal 2006).

5. Comparison of our model with experimental data and existing models

This section verifies our model with the experimental data discussed in section 3. Also, the present model is compared with the other existing models. We compute the numerical solution of equations (25) and (29) through the solution procedures explained in section 4. For the twelve experimental runs of Vanoni (1946) with particle diameter $D = 0.16$ mm, the

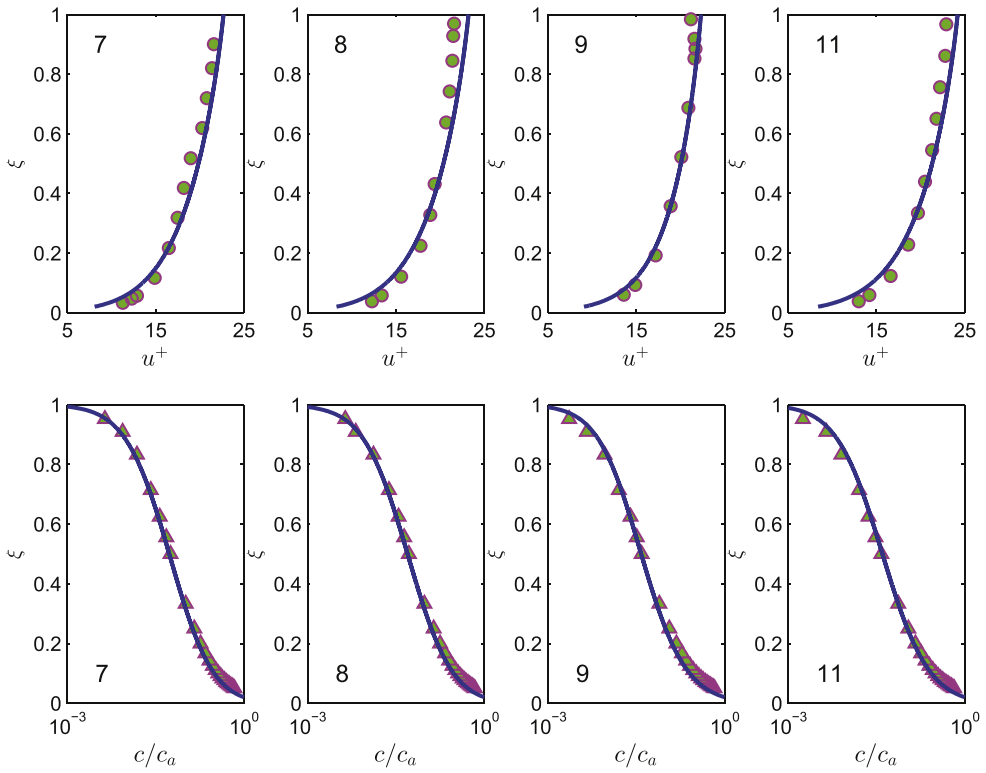

Figure 2. For experimental runs 7, 8, 9 and 11 of Vanoni (1946), comparison of u and c profiles between measured data (symbol) and computed values (solid line) from equations (25) and (29).

computed profiles of u^+ and c/c_a are plotted with the measured data in figures 1–3 where each figure shows four experimental runs together with their run names which are mentioned in table 1. Figure 4 depicts the comparison between measured data and computed u and c profiles for the remaining five experimental runs of Vanoni (1946) for $D = 0.10$ and 0.13 mm. We can observe from figures 1–4 that the computed profiles of u and c show good agreement with the observed data. The comparison analysis for the experimental data of Lyn (1988) is provided in figure 5 in which the first column stands for data over equilibrium bed and the remaining two columns represent data over starved bed. Figure 5 exhibits the good prediction accuracy of our model for Lyn (1988) data. We show the computed and measured profiles of u and c in figure 6 for three experimental runs of Xingkui and Ning (1989) and here also our model provides good agreement. Overall, we can assert that the proposed model shows good agreement with a wide range of experimental data.

Apart from the above discussed agreement analysis, we compare our model also with the other existing models. The traditional analytical equations on u and c profiles are log-law and Rouse equation respectively and hence we choose them for comparison. Moreover, it is worth mentioning that u and c profiles are studied simultaneously in this present study and therefore for comparison analysis, we need to select those models where u and c profiles were investigated together. We choose the theoretical models of Tsai and Tsai (2000), Mazumder

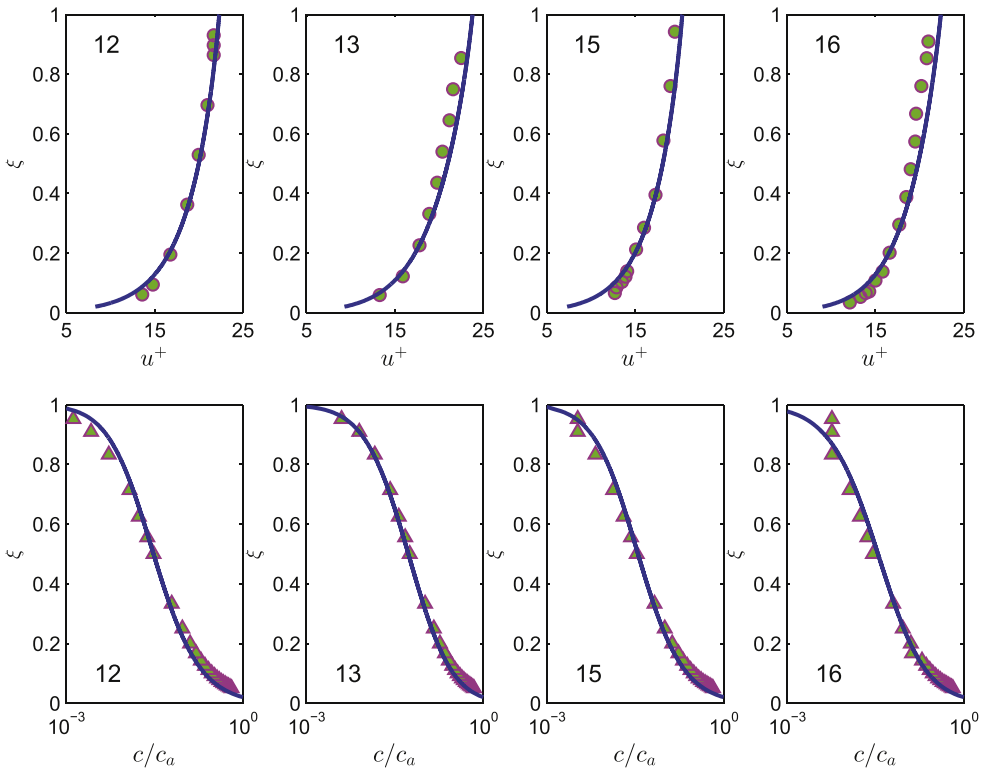

Figure 3. For experimental runs 12, 13, 15 and 16 of Vanoni (1946), comparison of u and c profiles between measured data (symbol) and computed values (solid line) from equations (25) and (29).

and Ghoshal (2002, 2006) and Yang (2007) which are based on mixing length approach except the last one where secondary current took the leading part. Strictly speaking, an infeasible space is required to show the graphical agreement between the twenty-three experimental runs selected in section 3 and the aforementioned models considered for the comparison with the present model. We perform the comparison study by a detailed error analysis and for this purpose, we select the following suitable error formula E which is the percentage of the mean of the relative errors

$$E = \frac{100}{N}\left[\sum_{i=1}^{N}\left|\frac{V_{\mathrm{ci}} - V_{\mathrm{oi}}}{V_{\mathrm{oi}}}\right|\right]. \tag{40}$$

For u and c profiles in an experimental run, the computed and the observed values of ith data point are represented by V_{ci} and V_{oi} respectively and N is the total number of data points in that run. The computed values of E for the present model and the other models considered are shown in table 2 where we represent the models of log-law and Rouse (1937) by $M1$, Tsai and Tsai (2000) by $M2$, Mazumder and Ghoshal (2002) by $M3$, Mazumder and Ghoshal (2006) by $M4$, Yang (2007) by $M5$ and present study by PM. The superscript star in table 2 represents the least value of errors computed from all models for the experimental run in that row. It is observed that our model shows minimum error for 17 experimental observations out of 23

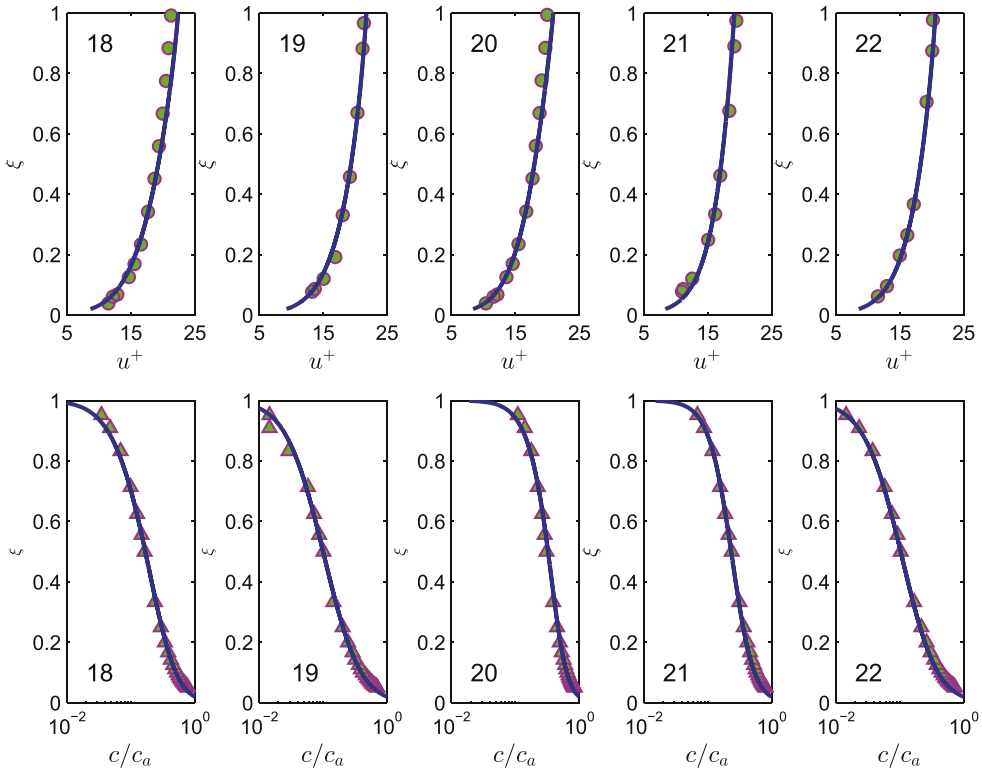

Figure 4. For experimental runs 18, 19, 20, 21 and 22 of Vanoni (1946), comparison of u and c profiles between measured data (symbol) and computed values (solid line) from equations (25) and (29).

experimental runs. This result proves the superior prediction accuracy of our model in comparison to the other existing models.

6. Discussions

Here, we first highlight the significance of the hydrodynamic mechanisms included in the model. After that, we show the contribution of our model to unveil the underlying physics of particle-turbulence interaction in the flow region. The section is followed by a vivid explanation on the advantages of our model in comparison to the existing ones.

6.1. Importance of hydrodynamic mechanisms included in the model

The significance of hydrodynamic mechanisms inserted in the model is discussed by studying the effects of secondary current, mixing length of sediment-laden flow and hindered settling as these turbulent features play an influential role in the mathematical modeling of this study. We randomly choose an experimental run from section 3 to get the values of all terms for the computation of u and c profiles from equations (25) and (29).

The impact of secondary current on u and c profiles is done by removing v_1 and v_2 in equations (25) and (29) as equation (12) displays that v is a summation of those two turbulent

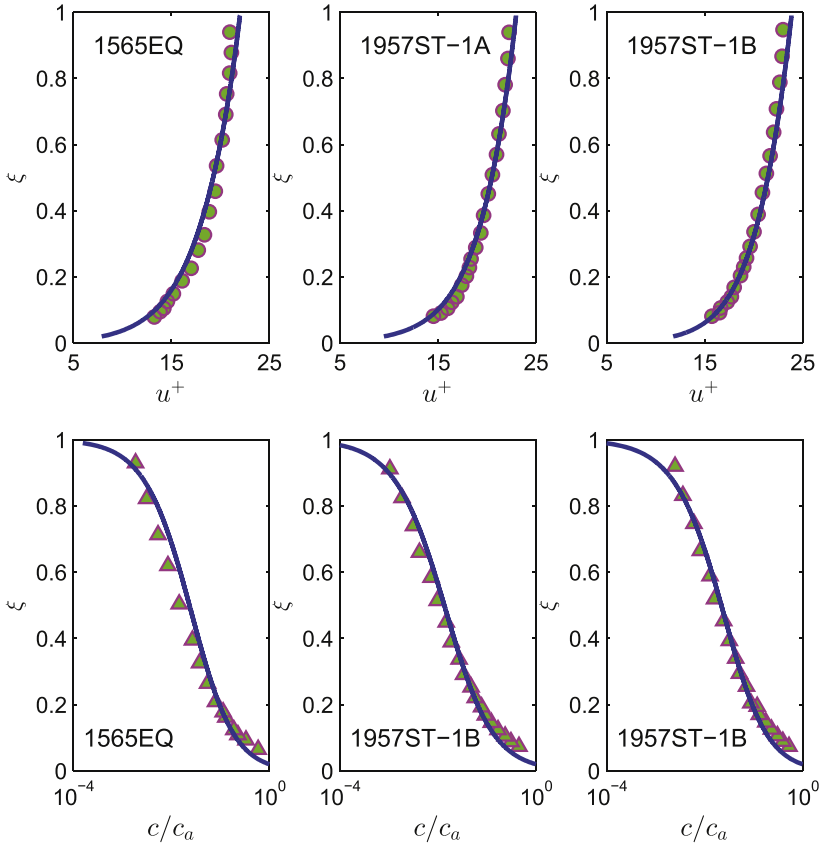

Figure 5. For experimental runs 1565EQ, 1957ST-1A and 1957ST-1B of Lyn (1988), comparison of u and c between measured data (symbol) and computed values (solid line) from equations (25) and (29).

components. We observe from figure 7 that u increases and c decreases in presence of secondary current in terms of v_1 and v_2. The explanation can be provided as follows. The secondary current follows a circular path along the cross-sectional area of an open channel and due to this circular motion, the magnitude of the vertical velocity of v increases with increasing lateral distance from the central region to the sidewall. The circular motion causes v at the middle region to carry out the sediment from there to the adjacent region along the lateral direction. The magnitude of v at that adjacent region is higher and it again carries out sediment near the sidewall through lateral transport and this successive transfer of particles goes on along the transverse direction. The concentration of sediment at the middle region of open channel decreases due to this transportation mechanism of particles. On the other hand, if v is having a decreased magnitude at the mid-section, an increased magnitude of u is obtained there as an equilibrium state always occurs in the flow region.

Prior to the published expression on the mixing length l of sediment-laden flow, researchers used the mixing length for particle free flow which can be obtained by putting $\lambda_2 = 0$ in equation (20). We can follow from figure 8 that the magnitudes of computed u and c profiles show increasing and decreasing characteristics respectively due to considering the mixing length of sediment-laden flow. The presence of suspended particles obstructs the

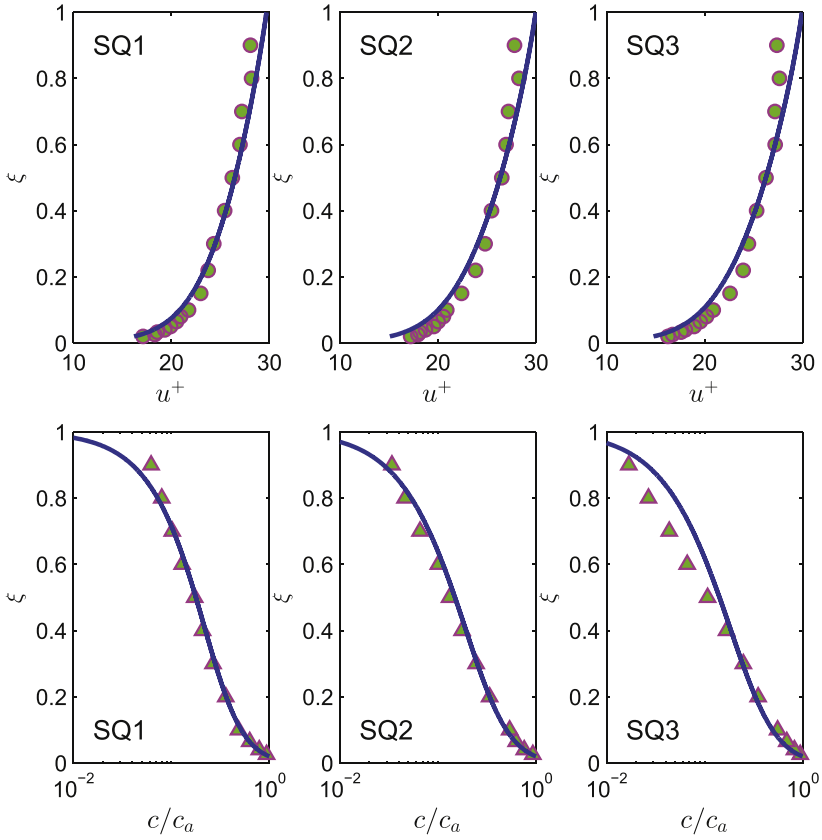

Figure 6. For experimental runs SQ1, SQ2 and SQ3 of Xingkui and Ning (1989), comparison of u and c between measured data (symbol) and computed values (solid line) from equations (25) and (29).

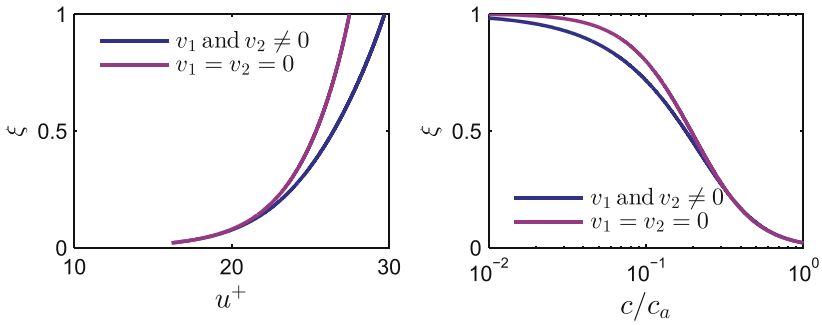

Figure 7. Influence of secondary current in terms of v_1 and v_2 on computed u and c profiles from equations (25) and (29).

vertical motion of fluid and results less transfer of fluid and sediment at upper layer than its lower layer for a particular flow depth in the flow region. The less vertical transportation of

Table 2. Calculated values of E from different models.

Run	M1	M2	M3	M4	M5	PM
			Vanoni (1946)			
1	20.9	*4.6	7.1	*4.6	6.5	11.4
3	45.7	15.7	12.8	15.3	13.4	*11.4
5	61.0	31.0	17.0	31.3	17.6	*11.0
6	55.5	30.1	15.8	30.4	16.3	*10.4
7	59.1	26.2	16.3	26.5	16.9	*10.5
8	69.6	33.6	19.6	34.0	20.0	*11.5
9	43.8	41.2	*10.3	42.0	18.3	15.6
11	133.7	72.8	49.7	74.2	51.3	*13.8
12	72.3	72.1	26.2	73.4	36.7	*20.5
13	64.6	30.9	27.2	31.5	25.8	*10.8
15	40.4	72.7	*11.3	73.7	20.1	16.0
16	41.4	62.2	18.0	62.8	67.2	*15.5
18	40.6	11.8	11.7	12.1	*5.3	*5.3
19	35.5	13.9	10.0	14.4	*5.2	7.1
20	21.7	5.2	4.3	5.3	4.8	*3.8
21	22.6	6.5	12.6	6.5	9.7	*5.5
22	23.9	10.5	13.1	10.9	*4.2	7.4
			Lyn (1988)			
1565EQ	75.8	71.0	38.6	61.5	60.9	*15.8
1957ST-1A	48.4	48.2	20.6	45.0	63.3	*12.1
1957ST-1B	78.2	27.8	17.1	28.6	30.4	*11.9
			Xingkui and Ning (1989)			
SQ1	14.3	4.9	10.4	*4.0	15.4	5.0
SQ1	47.5	11.8	17.3	14.8	11.2	*7.0
SQ2	101.2	23.2	42.5	30.9	16.2	*15.3

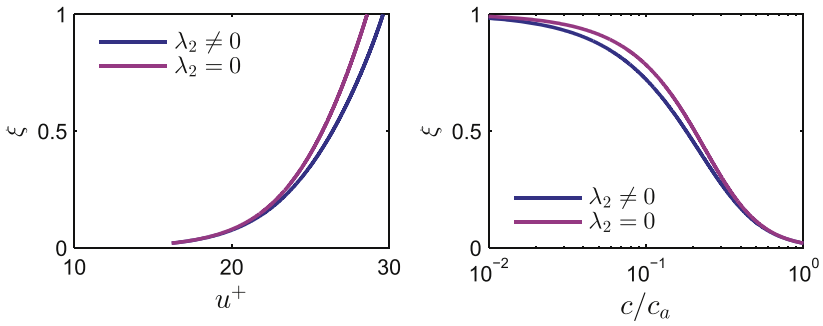

Figure 8. Influence of mixing length of sediment-laden flow in terms of λ_2 on computed u and c profiles from equations (25) and (29).

fluid and sediment causes increased and decreased magnitudes of u and c profiles respectively with increasing flow depth from the channel bed.

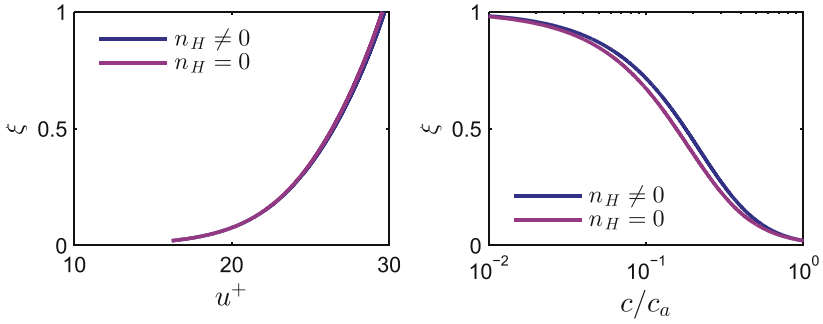

Figure 9. Influence of hindered settling in term of n_H on computed u and c profiles from equations (25) and (29).

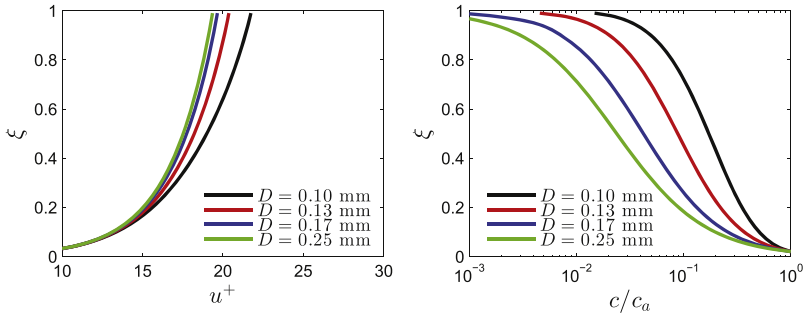

Figure 10. Effect of particle diameter D on computed u and c profiles from equations (25) and (29).

The influence of hindered settling on u and c profiles is performed by vanishing n_H in equations (25) and (29). We can notice from figure 9 that the magnitude of concentration profile increases due to the effect of hindered settling though negligible variation is observed for u profile. The settlement rate of a particle along vertical downward direction is prevented by other suspended particles in flow region owing to the hindered settling mechanism. Since the suspended particles obstruct their downward settlements between themselves, therefore an equilibrium settlement might occur throughout the flow region. This equilibrium mechanism has no significant effect on the dynamics of fluid in flow region and therefore u profile does not show any noticeable variation.

6.2. Contribution to reveal real phenomena of particle-turbulence interaction

Here we discuss the contribution of our model to unleash the underlying physics of particle-turbulence interaction throughout the flow region. This task is done as follows. We calculate u and c profiles through equations (25) and (29) like section 6.1. Then we observe the effects of different flow components on our model and investigate the ability of observed characteristics of u and c profiles to rationalize the phenomena of velocity and concentration occurring in reality. In this context, we intend to examine the effects of particle diameter D, mass density ρ_p of particle, fluid flux through shear velocity u_*, strength of secondary current in terms of λ_1 and intensity of mixing length by λ_2 as they show their noticeable contribution in the entire

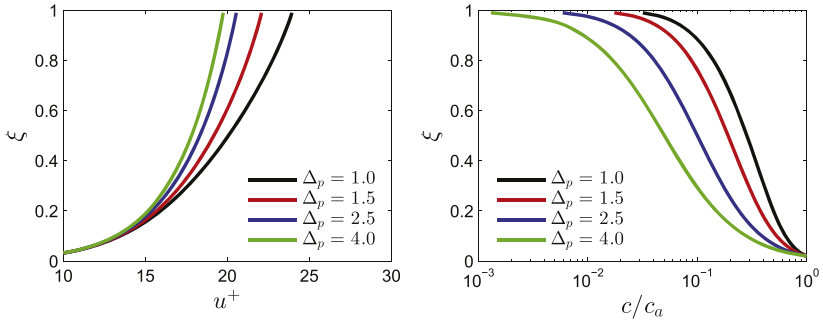

Figure 11. Effect of mass density of sediment particle in terms of Δ_p on computed u and c profiles from equations (25) and (29).

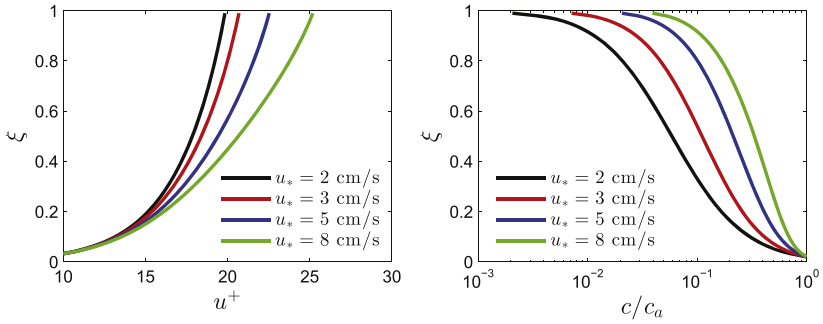

Figure 12. Effect of fluid flux in terms of shear velocity u_* on computed u and c profiles from equations (25) and (29).

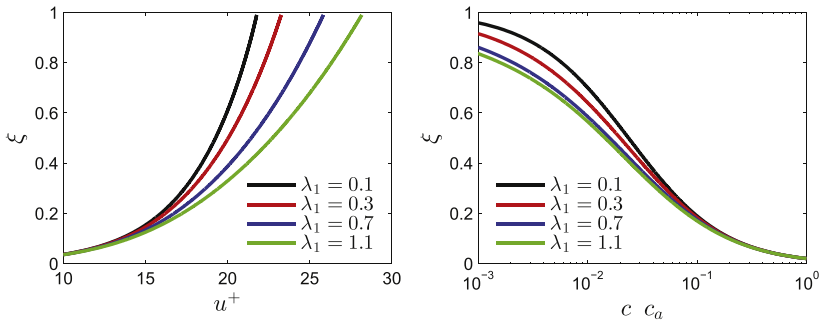

Figure 13. Effect of strength of secondary current v in terms of λ_1 on computed u and c profiles from equations (25) and (29).

mathematical modeling discussed in section 2. To study the impacts of those flow components, we vary the value of each of them by keeping the others constant.

The effect of particle diameter D on equations (25) and (29) is depicted in figure 10. It is followed that u and c increase with decreasing D. The size and weight of a particle decrease with decreasing D and therefore more sediment particles entrain into suspension due to their

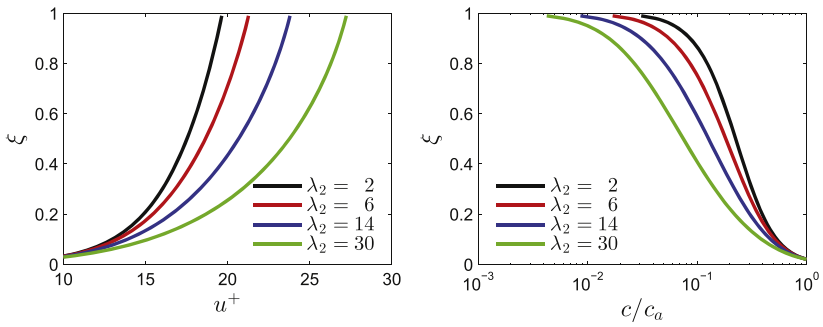

Figure 14. Effect of intensity of mixing length l in terms of λ_2 on computed u and c profiles from equations (25) and (29).

smaller size and weight. This increased concentration owing to more entrainment weakens the vertical momentum flux and results increased magnitude of u.

In figure 11, we display the effect of mass density ρ_p of particle in terms of Δ_p on the computed u and c profiles. We observe increasing nature of both profiles with decreasing Δ_p. The mass of particle decreases with decreasing Δ_p and therefore more amount of particles enter into suspension. This increased concentration enhances the value of u and the reason is already mentioned in the aforementioned paragraph.

We show the effect of fluid flux in terms of shear velocity u_* on the suggested model in figure 12 where each profile of u is normalized by the corresponding u_* assumed. We notice that u and c profiles increase with increasing u_* which increases with increasing fluid shear stress generated from the increasing fluid flux. This increased shear stress lifts more particles from the channel bed to suspension and results an increasing behavior of c.

The effect of the strength of secondary current in terms of λ_1 is illustrated in figure 13 where u increases and c decreases with increasing λ_1. In an open channel, v carries out sediment from the central region to the sidewall along the lateral direction and the mechanism is explained already in the second paragraph of section 6.1. The increased magnitude of v with increasing λ_1 is responsible for more lateral transportation of sediment and this fact results decreasing nature of c at the central region. On the other hand, as v plays less dominating role at the central region with increasing λ_1, an equilibrium state is maintained in the flow by the increased profile of u at that region.

Figure 14 demonstrates the influence of intensity of mixing length l through λ_2. We notice that u increases and c decreases with increasing λ_2. It is followed from equation (20) that the mixing length decreases with increasing λ_2 for a particular normalized vertical height ξ. This implies that the fluid located at that ξ moves less along vertical direction y and this reduced movement could be responsible for the increasing nature of u. In addition, due to the incompressible nature of fluid and solid phases during flow, the exchange rate of those phases along y direction maintains equilibrium by interchanging the equivalent amount of fluid and sediment. The less movement of fluid along y direction is responsible for getting less amount of sediment by exchanging method and results decreasing magnitude of c.

Towards the end of this section, we can ensure that our model has remarkable contribution to reveal particle-turbulence interaction in the flow region as well as to explain real phenomena of u and c profiles in terms of their impacts on each other in open channel turbulent flow laden with sediment.

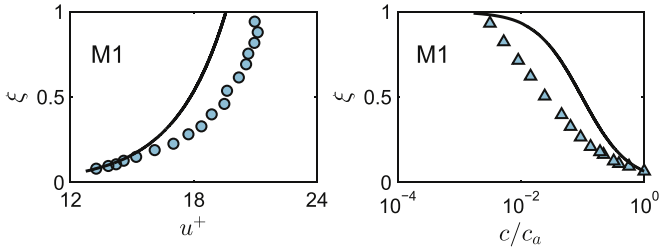

Figure 15. Comparison of run 1565EQ (symbol) of Lyn (1988) with computed u and c profiles (solid line) from model M1 of log-law and Rouse equation.

6.3. Significance of this research

Here we demonstrate the significance of our present research in comparison to the existing pertinent literature from several points of view. This demonstration is organized as follows. First, we discuss the novelty and the main attribute of our model. Next, we interpret the relevance of the co-existence of hydrodynamic mechanisms included in the model. At last, the advantages on the applicability of our model to predict u and c profiles are explained.

To explain the novelty of the present model, first it is worth mentioning that researchers (Umeyama 1992, Umeyama and Gerritsen 1992, Guo and Julien 2001, Huang *et al* 2008, Yang 2009, Kundu and Ghoshal 2012, Ghoshal and Kundu 2013, Kundu and Ghoshal 2013, 2014) have a propensity to do investigation either on u or on c profile and the indubitable reason to avoid the simultaneous computation of those profiles together with their impacts on each other is the intricate tangle of particle and fluid in the turbulent region. It has been acquainted from a profound inspection that those literature did not examine the underlying physics of u and c profiles in the domain of flow. Moreover, due to the negligence of either u or c profile, those models are constrained by insufficient consideration of flow physics. Unlike those models, here we study u and c profiles simultaneously as they interact between themselves during flow. Prior to our model, researchers (Tsai and Tsai 2000, Mazumder and Ghoshal 2002, Ghoshal and Mazumder 2005, Mazumder and Ghoshal 2006) studied u and c profiles together by considering only some specific effects of turbulence. The main limitation of those models is that they avoided the modern interpretation of turbulent features by considering hindered settling as a function of particle Reynolds number Re (Tsai and Tsai 2000, Mazumder and Ghoshal 2002, Ghoshal and Mazumder 2005, Mazumder and Ghoshal 2006), mixing length as a linear function of vertical height from the channel bed (Yang 2007), questionable expression of v_1 (Yang 2007) etc. Section 2 shows that our model includes the effects of secondary current in terms of the vetical velocity of fluid, additional vertical velocity of fluid due to suspended particles, mixing length of sediment-laden flow and hindered settling phenomenon together with their modern interpretations and corresponding mathematical equations. Unlike the previous researchers, an important nature in our modeling is that the turbulent features v_1, v_2, l, n_H, ϵ_s, ϵ_m and κ_m inserted in the present model vary with particle concentration. Those turbulent features and other turbulent components ω_p, y_o, τ_{*c} and c_a required to solve the model are derived by either theoretical or semitheoretical approach. Each of those features shows reasonable estimation accuracy for a wide region on the corresponding turbulent element. So, the novelty of our model in comparison to the existing ones is asserted by its generalized structure through the inclusion of modern expressions of several hydrodynamic mechanisms and turbulent components simultaneously.

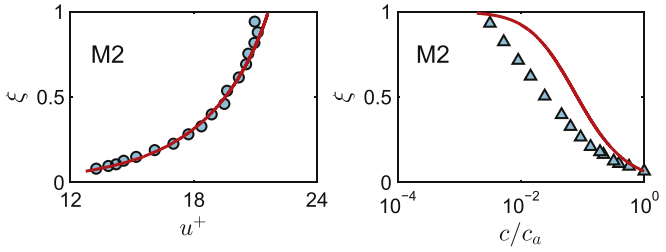

Figure 16. Comparison of run 1565EQ (symbol) of Lyn (1988) with computed u and c profiles (solid line) from model M2 of Tsai and Tsai (2000).

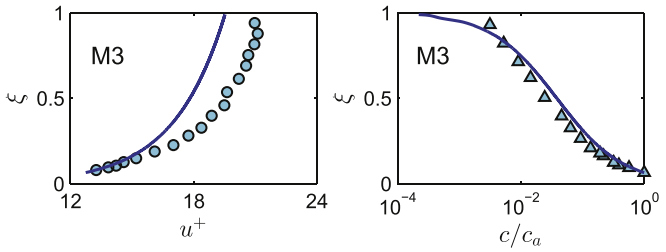

Figure 17. Comparison of run 1565EQ (symbol) of Lyn (1988) with computed u and c profiles (solid line) from model M3 of Mazumder and Ghoshal (2002).

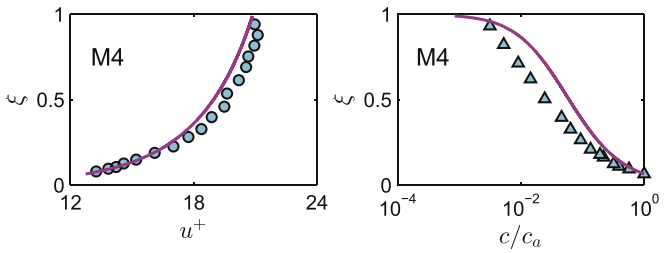

Figure 18. Comparison of run 1565EQ (symbol) of Lyn (1988) with computed u and c profiles (solid line) from model M4 of Mazumder and Ghoshal (2006).

Strictly speaking, previous literature (Tsai and Tsai 2000, Mazumder and Ghoshal 2002, Ghoshal and Mazumder 2005, Mazumder and Ghoshal 2006, Yang 2007) showed no enthusiasm to examine the particle-turbulence interaction by their models. In sharp contrast to them, sections 6.1 and 6.2 show remarkable contribution to uncover several phenomena of particle-turbulence interaction with accurate justification. This ability establishes the main attribute of our model in comparison to the others.

After the elucidation of novelty and greatness, we explain the pertinence of the co-existence of hydrodynamic mechanisms included in the model. We accomplish this task through a brief agreement analysis of an experimental run with models M1–M5 and PM. Our model gives least error for seventeen experimental runs in table 2 and out of them, we arbitrarily select a run 1565EQ of Lyn (1988) to perform the agreement analysis. We notice from figure 15 that the traditional log-law and the Rouse equation given by model M1 cannot predict the measured data of u and c respectively. The major two reasons behind this

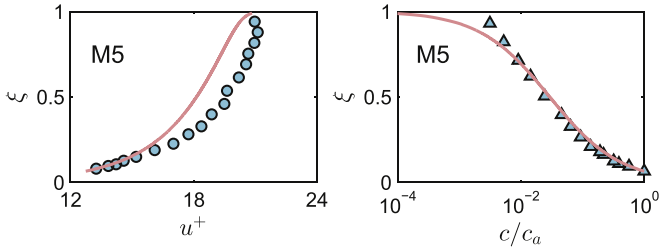

Figure 19. Comparison of run 1565EQ (symbol) of Lyn (1988) with computed u and c profiles (solid line) from model M5 of Yang (2007).

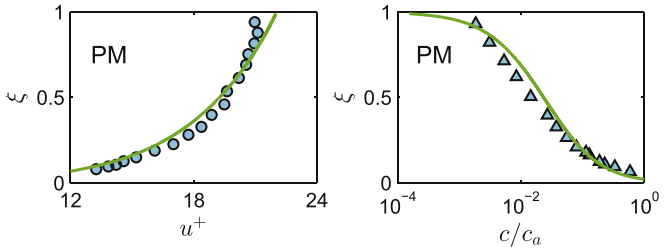

Figure 20. Comparison of run 1565EQ (symbol) of Lyn (1988) with computed u and c profiles (solid line) from present model PM given by equations (25) and (29).

phenomenon are that the negligence of various crucial turbulent effects during mathematical formulation and several assumptions for getting simple analytical structure of equations. Though model M2 of Tsai and Tsai (2000) shows good agreement with the measured u data in figure 16, but it overestimates c data and perhaps the reason is not considering the secondary current which can transport sediment from the central region to the sidewall through the cross-sectional area. Figure 17 depicts that model M3 of Mazumder and Ghoshal (2002) provides good estimation accuracy in the determination of c data though it underestimates u data. The occurrence of deviation might be due to considering the mixing length l of particle free flow and therefore the movement of fluid along vertical direction in the presence of suspended particles is not accounted properly through this model. Model M4 of Mazumder and Ghoshal (2006) exhibits differences between computed and observed values of u and c profiles in figure 18. This fact once again arises the question on the inclusion of secondary current in mathematical modeling as model M4 avoided this turbulent feature. Model M5 of Yang (2007) inserted the effect of secondary current albeit figure 19 exhibits good agreement for c data only. The probable cause is the consideration of linear profile of mixing length and questionable expression of v_1 by $uv_1/u_*^2 \propto -\xi$ which violates the modern fact that $v_1 = 0$ at $\xi = 1$ (Yang 2005, Yang *et al* 2012). On the contrary of the above mentioned disagreement, figure 20 illustrates good agrement between computed u and c profiles by our model PM and measured data. Hence, we claim that the co-existence of turbulent features included in our model is an indispensable combination to predict u and c profiles more accurately.

To demonstrate the importance of a model, it needs to mention the advantages of its applicability in comparison to existing ones. Unlike the previous literature (Tsai and Tsai 2000, Mazumder and Ghoshal 2002, Ghoshal and Mazumder 2005, Mazumder and Ghoshal 2006, Yang 2007), we investigate the accuracy of our model in section 5 to estimate

experimental data in comparison to the existing ones through a detailed error analysis. We visualize the superior prediction ability of our model from the computed errors in table 2 and this fact undoubtedly allows the researchers to apply the present model in the computation of u and c profiles. Besides this, from the experimental data, previous investigators (Tsai and Tsai 2000, Mazumder and Ghoshal 2002, 2006, Yang 2007) considered the reference level a which is placed a bit far from the channel bed and obtained the values of reference velocity u_a and reference concentration c_a at that point through either extrapolation or interpolation. The consideration of boundary condition in those models is not reasonable because it violates the physical definition of a, u_a and c_a since the thickness a of bed load layer is very thin and is located very near to the bed. On the other hand, this present study takes a as $0.02h$ which is a quite logical and calculates reasonable value of c_a from equation (37) given by Cao (1999). Consequently, the benefit to apply our model is that it is independent on experimental data for getting the values of a and c_a. Another drawback to apply the previous models is the estimation of several empirical parameters from experimental data like u_a, c_a, λ_2 in Tsai and Tsai (2000); u_a, κ, β in Mazumder and Ghoshal (2002); u_a, κ, β, λ_2 in Mazumder and Ghoshal (2006); u_a, c_a, β, λ_1 in Yang (2007) etc. In our model, we estimate only u_a and λ_2 from the experimental data and it helps to predict u and c profiles more easily. We also want to apprise that our model shows consistent behavior and pattern in section 6.2 for a broad range of different flow components. For the aforementioned advantages, we can disseminate the applicability of the present model for a wide applicable region to compute u and c profiles in sediment-laden open channel turbulent flow.

Towards the end, we want to mention two minor limitations of the present model. Though the obtained estimated values of λ_2 in table 1 agree with the available range in existing literature (Umeyama and Gerritsen 1992, Umeyama 1992, Tsai and Tsai 2000, Ghoshal and Mazumder 2005, Mazumder and Ghoshal 2006), but we are unable to find any global character on this parameter due to the variations of D, h, u_* etc at a time with varying experimental runs. In addition, we neglect the magnitude of lateral variation in comparison to that of vertical variation as we focus on u and c profiles at the central region of the open channel through the cross-sectional area. The present model could be improved further by considering lateral variation; however, the verification of that model would not be possible at present as relevant experimental data on the lateral variations of u and c profiles in open channel flow is still lacking in literature. Finally, we can say that the present study is significant in terms of its novelty, contribution and wide applicability in the field of fluvial sediment transport.

7. Conclusions

In this study, a generalized theoretical model is proposed to compute the vertical distribution of streamwise fluid velocity and particle concentration in open channel turbulent flow. The model is derived based on the Reynolds averaged Navier–Stokes equation and the mass conservation equation of solid and fluid phases and it includes the effects of secondary current in terms of the vertical velocity of fluid, additional vertical velocity of fluid due to the presence of sediment particles in suspension, mixing length of sediment-laden flow and settlement of the suspended sediment due to gravitational force. The significance of hydrodynamic mechanisms included in the model and the importance of their co-existence to predict velocity and concentration profiles are explained. The model shows good agreement with a wide range of experimental data and provides superior prediction accuracy in comparison to the other existing models. The proposed model has made a significant contribution

to explore several latent phenomena of particle-turbulence interaction in the flow region. The aforementioned abilities assert that the present model can be applicable to predict fluid velocity and particle concentration for a wide region of sediment-laden open channel turbulent flow.

References

Absi R 2011 An ordinary differential equation for velocity distribution and dip-phenomenon in open channel flows *J. Hydraul. Res.* **49** 82–9

Ahrens J P 2000 A fall-velocity equation *J. Waterw. Port Coast. Ocean Eng.* **126** 99–102

Cao Z 1999 Equilibrium near-bed concentration of suspended sediment *J. Hydraul. Eng.* **125** 1270–8

Castro-Orgaz O, Giraldez J V, Mateos L and Dey S 2012 Is the von Karman constant affected by sediment suspension? *J. Geophys. Res.: Earth Surf.* **117** 1270–8

Cellino M and Graf W H 1999 Sediment-laden flow in open-channels under noncapacity and capacity conditions *J. Hydraul. Eng.* **125** 455–62

Cheng N S 1997a Effect of concentration on settling velocity of sediment particles *J. Hydraul. Eng.* **123** 728–31

Cheng N S 1997b Simplified settling velocity formula for sediment particle *J. Hydraul. Eng.* **123** 149–52

Garcia M and Parker G 1991 Entrainment of bed sediment into suspension *J. Hydraul. Eng.* **117** 414–35

Garside J and Al-Dibouni M R 1977 Velocity-voidage relationships for fluidization and sedimentation in solid–liquid systems *Ind. Eng. Chem. Process Des. Dev.* **16** 206–14

Ghoshal K and Kundu S 2013 Influence of secondary current on vertical concentration distribution in an open channel flow *ISH J. Hydraul. Eng.* **19** 88–96

Ghoshal K and Mazumder B S 2005 Sediment-induced stratification in turbulent open-channel flow *Environmetrics* **16** 673–86

Guo J 2002 Logarithmic matching and its applications in computational hydraulics and sediment transport *J. Hydraul. Res.* **40** 555–65

Guo J and Julien P Y 2001 Turbulent velocity profiles in sediment-laden flows *J. Hydraul. Res.* **39** 11–23

Herrmann M J and Madsen O S 2007 Effect of stratification due to suspended sand on velocity and concentration distribution in unidirectional flows *J. Geophys. Res.: Oceans* **112** c02006

Huang S, Sun Z, Xu D and Xia S 2008 Vertical distribution of sediment concentration *J. Zhejiang Univ. Sci.* A **9** 1560–6

Imamoto H and Ishigaki T 1988 Measurement of secondary flow in an open channel *Proc. 6th IAHR-APD Cong.* pp 513–20

Jimenez J A and Madsen O S 2003 A simple formula to estimate settling velocity of natural sediments *J. Waterw. Port Coast. Ocean Eng.* **129** 70–8

Kinoshita R 1967 An analysis of the movement of flood waters by aerial photography: concerning characteristics of turbulence and surface flow *Photogr. Surv.* **6** 1–7

Kundu S and Ghoshal K 2012 An analytical model for velocity distribution and dip-phenomenon in uniform open channel flows *Int. J. Fluid Mech. Res.* **39** 381–95

Kundu S and Ghoshal K 2013 An explicit model for concentration distribution using biquadratic-log-wake law in an open channel flow *J. Appl. Fluid Mech.* **6** 339–50

Kundu S and Ghoshal K 2014 Effects of secondary current and stratification on suspension concentration in an open channel flow *Environ. Fluid Mech.* **14** 1357–80

Lyn D A 1988 A similarity approach to turbulent sediment-laden flows in open channels *J. Fluid. Mech.* **193** 1–26

Mazumder B S and Ghoshal K 2002 Velocity and suspension concentration in sediment-mixed fluid *Int. J. Sediment. Res.* **17** 220–32

Mazumder B S and Ghoshal K 2006 Velocity and concentration profiles in uniform sediment-laden flow *Appl. Math. Modelling* **30** 164–17

Muste M and Patel V C 1997 Velocity profiles for particles and liquid in open-channel flow with suspended sediment *J. Hydraul. Eng.* **123** 742–51

Nezu I 2002 Open-channel turbulence and its research prospect in the new century *Proc. 13th IAHR-APD Cong.* pp 8

Nezu I and Nakagawa H 1984 Cellular secondary currents in straight conduit *J. Hydraul. Eng.* **110** 173–93
Ohmoto T, Cui Z and Hirakawa R 2004 Effects of secondary currents on suspended sediment transport in an open channel flow *Int. Symp. Shallow Flows* pp 511–6
Pal D and Ghoshal K 2013 Hindered settling with an apparent particle diameter concept *Adv. Water. Resour.* **60** 178–87
Prandtl L 1932 Zur turbulenten Strdmung in Rohren und langs Platten *Ergebn. Aerodyn. Versuchsanst* **4** 18–29
Richardson J and Zaki W 1954 Sedimentation and fluidisation: I. *Trans. Inst. Chem. Eng.* **32** 35–53
Rouse H 1937 Modern conceptions of the mechanics or fluid turbulence *Trans. Am. Soc. Civ. Eng.* **102** 463–505
Smith J D and McLean S R 1977 Spatially averaged flow over a wavy surface *J. Geophys. Res.* **82** 1735–46
Soulsby R L and Whitehouse R J S 1997 Threshold of sediment motion in coastal environments *Proc. Combined Australasian Coast. Eng. Port Conf.* pp 149–54
Tsai C H and Tsai C T 2000 Velocity and concentration distributions of sediment-laden open channel flow *J. Am. Water Resour. Assoc.* **36** 1075–86
Umeyama M 1992 Vertical distribution of suspended sediment in uniform open-channel flow *J. Hydraul. Eng.* **118** 936–41
Umeyama M and Gerritsen F 1992 Velocity distribution in uniform sediment-laden flow *J. Hydraul. Eng.* **118** 229–45
van Rijn L C 1984 Sediment transport: II. Suspended load transport *J. Hydraul. Eng.* **110** 1613–41
Vanoni V A 1946 Transportation of suspended sediment by water *Trans. Am. Soc. Civ. Eng.* **111** 67–102
Villaret C and Trowbridge J H 1991 Effects of stratification by suspended sediments on turbulent shear flows *J. Geophys. Res.: Oceans* **96** 10659–80
Wang Z Q and Cheng N S 2005 Secondary flows over artificial bed strips *Adv. Water Resour.* **28** 441–50
Wang Z Q and Cheng N S 2006 Time-mean structure of secondary flows in open channel with longitudinal bedforms *Adv. Water Resour.* **29** 1634–49
Xingkui W and Ning Q 1989 Turbulence characteristics of sediment-laden flow *J. Hydraul. Eng.* **115** 781–800
Yang S Q 2005 Interactions of boundary shear stress, secondary currents and velocity *Fluid Dyn. Res.* **36** 121–36
Yang S Q 2007 Turbulent transfer mechanism in sediment-laden flow *J. Geophys. Res.: Earth Surf.* **112** F01005
Yang S Q 2009 Influence of sediment and secondary currents on velocity *Water Manag.* **162** 299–307
Yang S Q, Tan S K and Lim S Y 2004 Velocity distribution and dip-phenomenon in smooth uniform open channel flows *J. Hydraul. Eng.* **130** 1179–86
Yang S Q, Tan S K and Wang X K 2012 Mechanism of secondary currents in open channel flows *J. Geophys. Res.: Earth Surf.* **117** F04014
Zhiyao S, Tingting W, Fumin X and Ruijie L 2008 A simple formula for predicting settling velocity of sediment particles *Water Sci. Eng.* **1** 37–43
Zhou D and Ni J 1995 Effects of dynamic interaction on sediment-laden turbulent flows *J. Geophys. Res.: Oceans* **100** 981–96
Zyserman J A and Fredsoe J 1994 Data analysis of bed concentration of suspended sediment *J. Hydraul. Eng.* **120** 1021–42